Environment, Development and Sustainability
https://doi.org/10.1007/s10668-021-01363-7

Multi-criteria analysis for mapping of environmentally sensitive areas in a karst ecosystem

Mudahir Ozgul[1] · **Turgay Dindaroglu**[2]

Received: 6 February 2020 / Accepted: 22 March 2021

Abstract
Karst ecosystems are one of the ecologically sensitive areas most affected by the dramatic harmful effects of the desertification process due to their structural, geomorphologic, and ecologic characteristics. The objective of this study was to assess and mapping ecologically sensitive areas (ESAs) for monitoring desertification and improving degraded forest areas in karst ecosystems. Sensitive ecological areas were evaluated using the Mediterranean Desertification and Land Use Methodology (MEDALUS) by considering soil quality, vegetation quality, climate quality, and management quality. Three new parameters (exposed rocky surface index, soil organic carbon index, and depression area index) were added specifically to karst ecosystem were evaluated using the Analytic Hierarchic Process (AHP) to determine ecological sensitivity. The study area is Sarimsak Karstic Mountain located in Andirin, Kahramanmaras. Soil organic carbon exposed rocky surface and depression area indices were evaluated over 110 soil samples. Values of each indices were determined according to the AHP methodology. The new $SQI_{modified}$ map, which was generated using new indices unique to karstic ecosystems provided a more precise spatial distribution. The results indicated that 44.49% of the study area is *Critical*, 51.94% is *Fragile*, and 3.58% is *Potential* in terms of desertification levels. In areas identified as *Critical*; agricultural fields, rangelands, and rocky surfaces cover 71.54%. Urban areas were evaluated as 100% *Fragile* class. Forested areas were evaluated in the *Fragile* and *Potential* class. The forest cover class affects *Fragile* and *Potential* status very closely. With the increase in forest cover rate, it has reduced fragility. The most critical ESAi classification area (C3) was detected in rangelands. Specific indices should be created to provide a realistic perspective in the combat to desertification in karst ecosystems.

Keywords Desertification · Sensitive areas · MEDALUS · AHP · Karst Ecosystems

✉ Turgay Dindaroglu
turgaydindaroglu@hotmail.com; turgaydindaroglu@ksu.edu.tr

[1] Faculty of Agriculture, Department of Soil Science and Plant Nutrition, Ataturk University, 25240 Erzurum, Turkey

[2] Faculty of Forestry, Department of Forest Engineering, Kahramanmaras Sutcu Imam University, 46100 Kahramanmaraş, Turkey

1 Introduction

Desertification is defined as "land degradation in arid, semi-arid and sub-humid regions affecting human activities and climate change and resulting from various factors" according to by the United Nations Convention to Combat Desertification (UNCCD, 1994). Desertification is a global issue that poses a threat to the environment's long-term sustainability, especially in arid areas (Salvati, 2014). Desertification is one of the threats to environmental sustainability. Environmental sustainability is linked to the balance between ecosystem dynamics and the quality of landscapes that contribute positively or negatively to the functioning of ecosystems (Zuindeau, 2007). Desertification brings many problems including food supply decline, poverty, creation of an unhealthy environment, and eventually migration (Rossi, 2020). Drought, deforestation, unplanned agricultural activities, overgrazing, urbanization and soil pollution, climate change etc., cause and accelerate desertification (Haktanır et al., 2004; Smith et al. 2019). Combating desertification is very important to preserving complex ecological relationships, as it affects the productivity of the soil. Therefore, identifying environmentally sensitive areas in terms of ecological relationships is very important (UNEP, 2007). Desertification processes can be caused by poor land management. The presence of a natural desert environment by itself cannot be considered an indicator of desertification. Unfortunately, data that need to follow desertification processes are limited. Whether desertification is permanent, as well as when and how it can be stopped are some of the questions that scientists are trying to answer (USGS 1997). Almost 71% of dryland areas all over the world are estimated to be at risk of desertification (Dregne & Chou, 1992). Desertification causes significant negative changes in the physical, chemical, and biological properties of the soil (Puigdefabregas, 1998; Okin et al., 2001; Gonzalez, 2001; Cabral et al., 2003; D'Antonio and Vitousek, 1992). With increasing droughts in the USA, southern Europe, the Mediterranean, and the Middle East, desertification is expected to have a significant effect on human movement (Seager, 2007). Some results of the conversion of natural vegetation to arable land are accelerated soil erosion and nutrient loss, which are important indicators of desertification (Okin et al., 2001; Sharma, 1998; Dismed, 2005).

Although karst areas are gaining importance because they have rich water and mineral resources, unique habitats and magnificent views (Veni et al., 2001; Febles et al., 2012; Peng et al., 2013; Bai et al., 2013) desertification effects due to incorrect land use and global warming in karstic regions, it has emerged as heavy soil erosion, and vegetation degradation (Guo et al., 2013). It is very important to evaluate the spatial distribution of desertification of karst ecosystems (Huand & Chai 2007). Xu and Zhang (2014) evaluated karst rocky desertification using such features as lithology, soil type, road buffer zone, physiographic factors, settlement influence, gross domestic product density, and population density. In some studies, it is claimed that extreme human pressure caused by agricultural activities in sloping areas may be responsible for rock desertification due to limited croplands in karst areas (Wu et al., 2011). The spatial traces of the karstic ecological corridors can be restored and rock desertification can be minimized in order to combat the inefficiency caused by the fragile karstic ecosystem (Dindaroglu, 2020).

Several models are used to assessed and monitored the vulnerability of desertification processes. In the Mediterranean region, the vulnerability of the land to desertification has been associated with drought, unsustainable land use, and ecological (edaphic, climatic, and topographic) conditions unique to the region (Feoli et al., 2003; Kosmas et al., 2000). Specific sensitive components of an ecosystem can accelerate desertification processes where they

originate (Akbari et al., 2020). The success of many methods aiming to combat desertification in practice depends on a good understanding of complex and variable environmental conditions (Botoni et al., 2010). The Mediterranean Desertification and Land Use model (MEDALUS) developed for the Mediterranean region was used in this research. The desertification sensitivity index is determined on the basis of main indicators such as soil, climate, vegetation and land management, and sub-indicators (Kosmas et al., 1999). In the Karst regions, the MEDALUS approach has also been used to detect environmental problems such as land desertification, soil erosion, soil salinization, and rock desertification (Liu et al., 2015). The MEDALUS approach is one of the most widely used methods for calculating the land's vulnerability to desertification. This approach allows land classification based on sensitivity level with flexible input variables (Ferrara et al., 2012) and sensitivity to different land degradation processes can be assessed (Besser & Hamed, 2021). In the world and Turkey, MEDALUS methods have new parameters are added or different methods to re-scoring studies. Symeonakis et al., (2014), assessment of ESAi on Lesbos Island (Greece), soil erosion, groundwater quality, etc., estimated through a modified ESAi with different parameters.

GIS is a highly preferred method in determining and monitoring desertification (Dindaroglu, 2015). GIS methods can reveal spatial information temporally, creating new and more sophisticated images that can aid decision-making. The characteristics of the lands can be determined precisely by using appropriate methods and using certain criteria (Griffiths & Dushenko, 2011). Many researchers have experienced that multi-criteria decision-making is a useful method for understanding complex ecological relationships in natural sciences. These models use an analytical hierarchy process (AHP) of Saaty (1990) to determine the relationship between soil and other ecological factors for sustainable environmental management (Agnihotri et al., 2021; Aksu & Küçük, 2020; Basu & Pal, 2020; Hornero et al., 2016; Jhariya et al., 2017). AHP is chosen because it can evaluate multiple data sets and makes the decision-making process more efficient by comparing each criterion pair-wise (Langemeyer et al., 2016). Budak et al., (2018) scored again MEDALUS indicators in a study conducted by the AHP method in Mesopotamia, Turkey.

Like every natural ecosystem, Karst ecosystems have complex ecological relationships. Although poor soil quality and scarce vegetation appear to be mainly the result of unstable ecological conditions, the contribution of unsustainable land use and poorly understood complex ecological relationships must also be demonstrated (Hamdouch & Zuindeau, 2010). Complex habitat factors need to be analyzed to determine the potential of ecosystems' available resources and environmental carrying capacities. These factors can directly or indirectly affect sustainable development. Therefore, enrichment of index systems of models such as resource and environmental carrying capacity and adaptive improvement of their application are the necessary steps for the sustainability of ecosystems (Zou & Ma, 2021). The aim of this study is to create spatially more precise models of ecological sensitivity specific to the karst ecosystem within the scope of combating desertification. For this purpose, some indicators specific to Karst ecosystems (soil organic carbon, depression area, and exposed surface rocky area) were added to the MEDALUS and the sensitivity of the new model was evaluated.

2 Material and method

This research was carried out around Sarimsak Mountain, which is located in the Mediterranean city of Kahramanmaraş, Turkey. The bounding geographical coordinates of the study area are 37°33′09′′–37°35′56′′ north latitude and 36°22′22′′–36°22′21′′ east longitude (Fig. 1). The research area covers 1431 hectares of land.

2.1 Climate, topograpy and geology

Sarımsak Mountain, which is the research area, has an average altitude of 1050 m (Dindaroglu and Vermez 2019). Located in the northeast of the Mediterranean region, Andirin district of Kahramanmaraş is located in the transition zone of Mediterranean climate and continental climate. It is seen that the hottest month in the region is August at 22.3 °C. It is seen that the coldest month is in February at 2.8 °C. Annual average rainfall is 1427 mm in Andirin. The least precipitation occurs in August with 14.9 mm (MGM, 2017).

According to Blumenthal, (1947), the presence of Upper Devonian, Permo-Carboniferous, Jurassic and Cretaceous rocks in the Andirin region was detected. Lithological formation of the area, the Cambrian process, and Paleozoic units began to be deposited. As a result, it was stated that it gained the present morphology with the Alpine Orogeny. The geological structure of the Andirin Sarımsak Mountain research area generally consists of limestone formations (Kozlu, 1987; Yilmaz ve Gurer 1996).

2.2 Method

2.2.1 Soil sampling

In total, 110 soil samples (0–20 cm depth) were collected from the study area by considering physiographic characteristics (two aspects and three altitudes) and land use types; forest (30), cropland (30), rangeland (30) rocky (10) and settlement (10).

According to site classification data (Dindaroglu and Vermez 2019), three altitude groups (870–1080 mt, 1080–1290 mt, 1290–1500 mt) and two aspect groups (South-West and North-East) were formed in the study area. Settlements are located in the 1st elevation group (870–1080 mt). Due to the distribution of rocky areas, soil sample intake was limited according to all altitude and aspect groups.

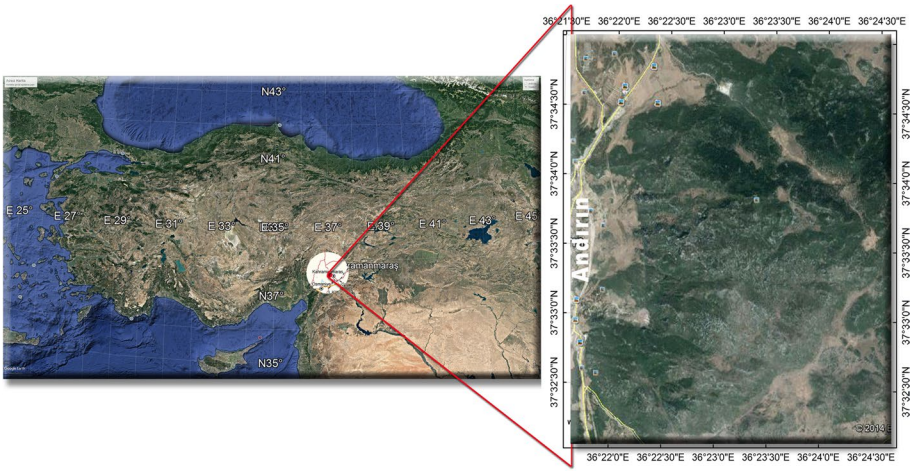

Fig. 1 Location maps of the research area

2.2.2 Soil analyses and other ESA indicators

MEDALUS includes many soil analysis and other quality parameters (Table 1). Within the scope of this study, the basic MEDALUS parameters were embedded in the original method by adding three new parameters specific to karstic ecosystems using AHP.

2.2.3 MESALUS concept; environmentally sensitive areas to desertification indices (ESAi)

Desertification potential was evaluated using the main ecological parameters; soil quality index, climate quality index, vegetation quality index and management quality index and their sub-parameters (Kosmas et al., 1999). Soil quality index (SQI) calculated using the following formula (1) (Kosmas et al., 1999).

$$\mathrm{SQI}_{\mathrm{original}} = (\mathrm{ST} * \mathrm{PM} * \mathrm{SLP} * \mathrm{SD} * \mathrm{DRJ})^{1/5} \quad (1)$$

where SQI is soil quality index, ST is soil texture, PM is parent material, SLP is slope, SD is depth of the soil horizon, DRJ is drainage. SQI values were determined for all 110-soil sampling points. Soil texture, parent material, soil depth, slope, and drainage were calculated using the methods indicated in Table 1.

Table 1 ESA indicators (ESAi)

Acronym	Meaning	Reference/Data sources
ST	Soil texture	Bouyoucos (1962)/Lab analyses
pH	Soil reaction	Gulcur (1974)/Lab analyses
SOC	Soil Organic Carbon	Walkley and Black (1934); Irmak (1954)/Lab analyses
PM	Parent Material	Blumenthal (1947)/Geology map
SD	Soil Depth	Gulcur (1974)/Field survey
STN	Stoniness	
DRJ	Drainage	
SLP	Slope Gradient	Digital surface map/SRTM data
ERS	Exposed Rocky Surface	Landsat 8 Satellite image/Field survey
DPRS	Depression area	Jenson and Domingue (1988)/D8 flow direction algorithm
RNF	Rainfall	Meteorological data (MGM, 2017)
ARD	Aridity	Meteorological data (MGM, 2017)
ASP	Aspects	Digital surface map
PCV	Plant Cover	Landsat 8 Satellite image and forest management map
EPR	Erosion Protection	Field survey
DRS	Drought Resistance	Meteorological data
FIR	Fire Risk	Forest management map
LU	Landuse	Landsat 8 Satellite image and forest management map
LUI	Landuse intensity	Field survey
POL	Policy	Field survey and forest management map

2.2.4 New modified SQI for specific karst ecosystem and analyzing of new Indices

Three specific new parameters; exposed rocky surface, soil organic carbon content, and depression areas were added into the soil quality index using the following formula (2) for the karst ecosystem (Fig. 2).

$$SQI_{modified} = (ST * PM * SLP * SD * DRJ * SOC * ERS * DPRS)^{1/8} \quad (2)$$

where SOC is soil organic carbon, ERS is exposed rocky surface and DPRS is depression area.

Exposed rocky surfaces (ERS) were obtained using the Landsat8 satellite images. Land cover/land use was determined in previous studies by Dindaroglu et al., (2019) using the "supervised" classification method. For various land uses in this study, different band combinations were used to identify areas of forest areas (6-5-4), urban areas (7-6-4), agricultural areas (6-5-2), and rock surface (7-6-2). The total number of spectral signatures for all educational areas was 270. Soil organic carbon (SOC) content was determined by the Walkley–Black method (Nelson & Sommers, 1996). Detection of depression areas (DEPRS) was defined using the D8 flow direction algorithm (Jenson & Domingue 1988) using ArcHydro module (ESRI, 2011; Maidment, 2002; Maidment & Djokic, 2000).

Karstic habitats such as doline, uvala are unique to these new criteria. It is due to the chemical and physical characteristics of the rocks that cause the formations to evaporate. Organic matter, which accumulates more in the areas of depression and cracks created as a consequence of the dissolution of these rocks, is the source of biodiversity. Since the depth of soil in karst areas is highly variable, soil usage is also affected. Therefore, it is important to expose the rocks (Dindaroglu et al., 2019).

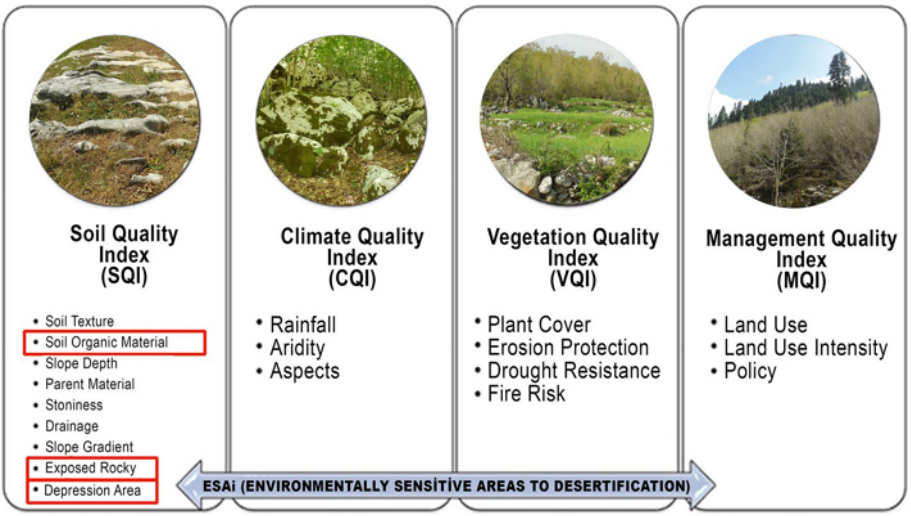

Fig. 2 ESAi methodology (Modified from Kosmas et al., 1999)

Environmentally Sensitive Areas index (ESAi) was determined using the soil quality index, climate quality index, vegetation quality index and management quality index using the following formula (3) (Kosmas et al., 1999).

$$\mathbf{ESAi} = (\mathrm{SQI} \times \mathrm{CQI} \times \mathrm{VQI} \times \mathrm{MQI})^{\mathbf{1/4}} \tag{3}$$

Type of ESAs values and ranges of indices are made according to the following classification system (Table 2).

The following symbols are used in the detailed mapping of ESAi (Table 3).

2.2.5 Evaluating of new indices with analytical hierarchy process (AHP)

Analytical Hierarchy Process (AHP), a method of estimating or determining weights based on decision hierarchy (Saaty, 1980), was used for obtaining the weights of the factors related to ESAi. AHP flow chart is given in Fig. 3.

The main factor in the comparison between the factors in the AHP model is a square matrix with *n*x*n* size as shown below (4).

$$A = \begin{bmatrix} a_{11} & a_{12} & \ldots & a_{1n} \\ a_{21} & a_{22} & \ldots & a_{2n} \\ . & & & . \\ . & & & . \\ . & & & . \\ a_{n1} & a_{n2} & \ldots & a_{nn} \end{bmatrix} \tag{4}$$

One-to-one mutual significance values are used to compare factors. The significance scale evaluated such as, 1; Equal importance of both factors, 3; Factor "a" is more important than factor "b", 5; Factor "a" is more important than factor "b", 7; Factor "a" has very strong importance compared to factor "b", 9; Factor "a" is of absolute superiority compared to factor "b" (Saaty, 1980).

The AHP software provided the consistency ratio (CR) was measured values. A coefficient called the Basic Value (**λ**) was used for CR calculation. Consistency Indicator (CI) can be calculated using the formula (5) (Saaty & Vargas, 1994).

Table 2 Types of ESAi and ranges of indices in the Karst ecosystem (Kosmas et al., 1999)

Type	Subtype	Range of ESAi
Critical	C3	> 1.53
Critical	C2	1.42–1.53
Critical	C1	1.38–1.41
Fragile	F3	1.33–1.37
Fragile	F2	1.27–1.32
Fragile	F1	1.23–1.26
Potential	P	1.17–1.22
Non affected	N	< 1.17

Table 3 Mapping symbols for ESAi to desertification (Kosmas et al., 1999)

Symbols										
F	1	–	c	2	s	1	v	2	m	1
ESAs type	ESAs subtype		Climate	Degree of limitation	Soil	Degree of limitation	Vegetation	Degree of limitation	Management	Degree of limitation

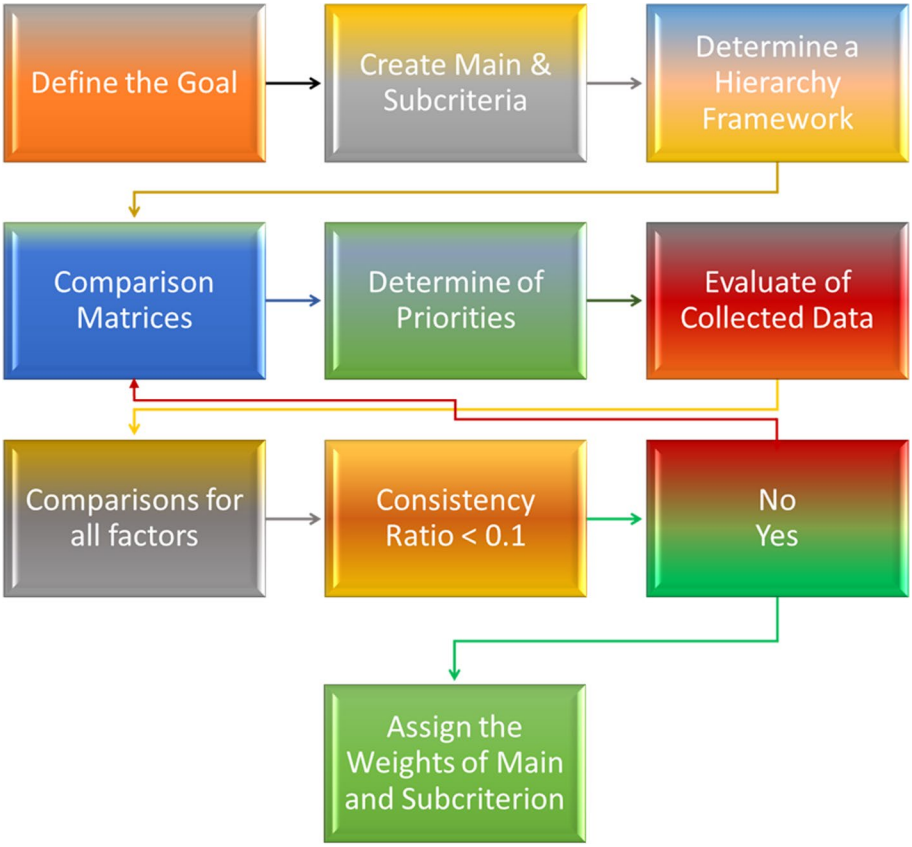

Fig. 3 AHP flow chart (Modified from Saaty, 1980)

$$\mathrm{CI} = \frac{\lambda - n}{n - 1} \tag{5}$$

Finally, CR formula (6) was measured using the CI is divided by Random Indicator (RI) standard correction value (Table 4).

Table 4 Random indicator (RI) values for AHP (Saaty, 1991)

N	RI	N	RI
1	0	8	1.41
2	0	9	1.45
3	0.58	10	1.49
4	0.90	11	1.51
5	1.12	12	1.48
6	1.24	13	1.56

$$CR = \frac{\mathrm{CI}}{\mathrm{RI}} \tag{6}$$

If CR value < 0.10 its means that the comparisons are consistent. If CR value > 0.10 indicates calculation error in inconsistency in AHP (Saaty, 1991). The AHP software program called "Super Decisions" (Saaty et al. 2019) was used to determine criterion weights and inconsistencies in this study.

For producing ESAs maps for the Karst ecosystem, the MEDALUS model supported by new indices was used after validating and assigning weights given in Table 5.

In determining SQI weights of SOC, ERS, and DPRS indices; $SQI_{original}$ maps and SOC, ERS, and DPRS maps are overlapped. The relationship values between SOC, ERS, DPRS and SQI are weighted by AHP. After calculating the new weight values of SOC, ERS, and DPRS, new maps were produced by using the $SQI_{modified}$ formula (2).

2.2.6 Geostatistical analysis

The "Kriging" interpolation technique was performed for geostatistical analysis using ArcGIS 10.1 software. Spatial analyses were carried out with prepared SQI, CQI, VQI, and MQI spatial distribution maps. The formula of Ordinary Kriging used in this study is as follows (7). The Ordinary Kriging method was preferred due to the sample distribution.

$$Z(\mathrm{S}_0) = \sum_{i=1}^{N} \lambda_i Z\left(\mathrm{S}_\mathrm{i}\right) \tag{7}$$

where

Z(s*i*); measured value at the location (*i*th),

λ_i; unknown weight (*i*th).

s_0; estimation location.

Unknown weights (λp) depend on the distance to the location of the unknown values and the spatial relationships between known values.

Generally, statistical model estimates unmeasured values using known values. Some differences occur between the true value $Z(s_0)$ and the predictor, $\sum\lambda_i Z(s_i)$, is as small as possible. To minimize the statistical prediction used the following formula (8),

$$\left[Z\left(\mathbf{S}_0\right) - \sum_{i=1}^{N} \lambda_i Z(\mathbf{S}_i)\right]^2 \tag{8}$$

The kriging interpolation technique is a very useful method to transfer data into GIS software to analyze areas that have no data. The models evaluated some criteria such as

Table 5 Evaluate of new indices by AHP

Definition of the goal	New factors for karst area	Alternatives
Adding new indices for MEDALUS using AHP	Soil Organic Carbon Depression Area Exposed Rocky	Very high High Medium Low

the average error (ME) and the square root of the estimated error of the mean standardized (RMSS) (Johnston et al., 2001).

3 Results and discussion

Descriptive statistics of some parameters used in SQI calculation are presented in Table 6. OM content ranged from 0.21 to 11.90%, Clay 8.57% to 62.00%, Silt from 0.66% to 35.55%, and sand from 17.10% to 90.77%.

3.1 Mapping of SOC content, depression area and exposed rocky surfaces

Soil organic carbon content within the study area changed between 0 and 9% (Fig. 4). In total, 3450 depression areas were identified, which is about 36% of the whole study area, using the ArcHydro module. These areas are of general climatic and physiographic characteristics suitable for soil formation and accumulation because of soil erosion (Fig. 5).

Using the supervised land cover classification, 281-exposed rocky areas were determined. The minimum exposed rocky area is 0.03 ha and the maximum exposed rocky area is 65.46 ha, with an average exposed rocky area of 0.96 ha. The total area occupied by exposed rocks is 267.50 ha (Fig. 6).

3.2 Evaluation of the new specific ESAs indices for karst ecosystem

In this AHP fiction, three factors (soil organic carbon, exposed surface rocks, and depression area) were identified have a very sensitive situations in the Karst area. For this purpose, data obtained from the field for these three new factors were entered into the AHP system using expert opinions. Because of AHP evaluation, consistency values, normalized and estimated values for these three factors are given in Figs. 7, 8 and 9.

According to the ESAs map, the exposed of rocky surfaces are classified in Table 7, soil organic carbon content is classified in Table 8 and depression areas are classified in Table 9.

The maps of soil quality index, climate quality index, vegetation quality index, and management quality index for evaluation of ESAs were produced using the Kriging method. The lowest error rate and strong spatial dependence models were selected and the maps of soil quality, climate quality, vegetation quality, and management quality were produced.

A circular model for soil quality index, an exponential model for vegetation quality index, and a spherical model for management quality index have been found to be suitable

Table 6 Descriptive analyses of the soils

	Minimum	Maximum	Mean	Std. Deviation	Skewness	Kurtosis
OM	0.21	11.90	5.44	3.11	0.220	−0.96
Clay	8.57	62.00	35.74	12.03	−0.119	−0.56
Silt	0.66	35.55	18.61	5.26	−0.114	1.44
Sand	17.10	90.77	45.64	14.95	0.474	−0.09

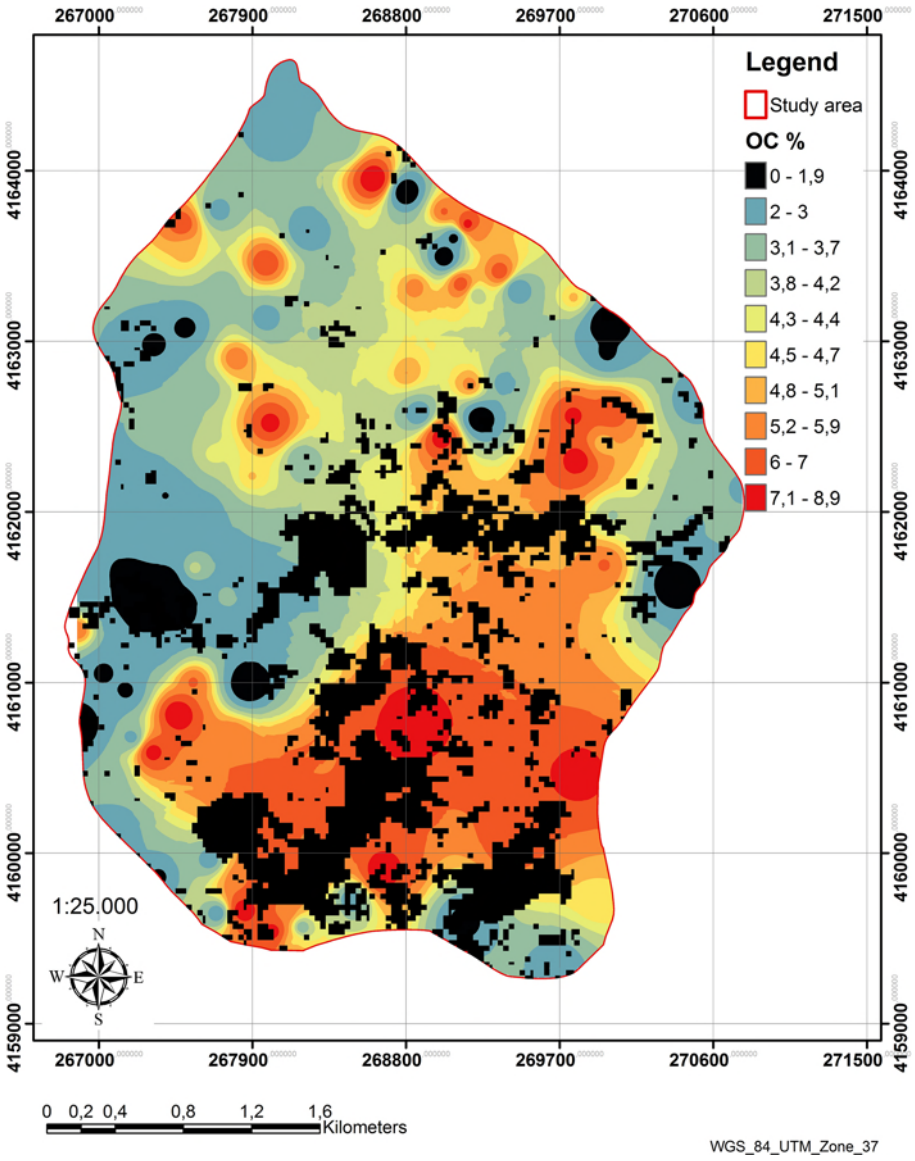

Fig. 4 Distribution of SOC content (%)

(Table 10). The mapping of SQI used in models is normal, mapping of VQI and MQI used in models has a strong spatial dependence (Table 9).

The $SQI_{original}$, $SQI_{modified}$, VQI, and MQI map are shown below (Figs. 10, 11, 13, and 14). The resolution of all maps is 30 m. In the soil quality index map, the deep and productive soil is seen in depression areas in karstic ecosystems. Soil depth is an important quality parameter in karstic ecosystems. Three indicators (SOC, ERS, and DPRS) specific to karstic ecosystems were added to the SQI calculation, the SQI distribution in the area also

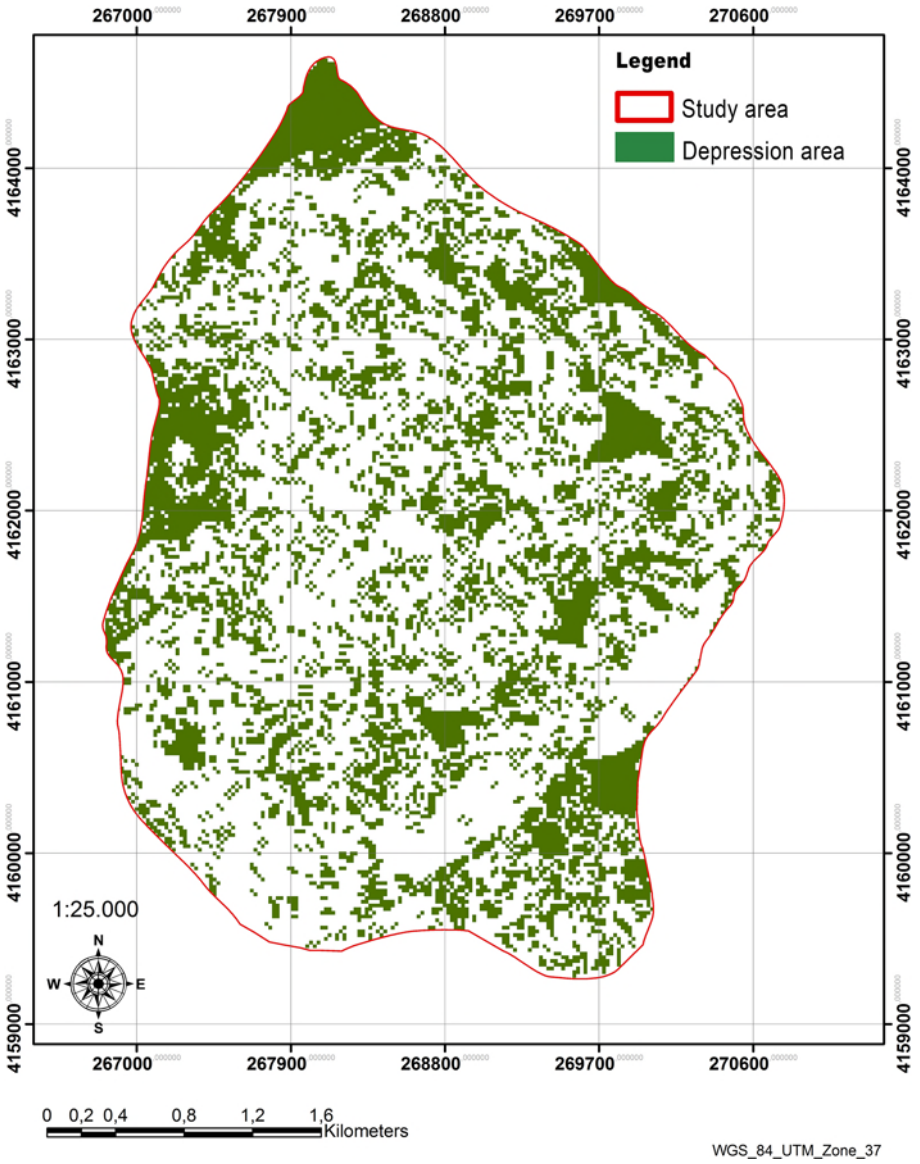

Fig. 5 Distribution of depression area

changed. The $SQI_{original}$ and $SQI_{Modified}$ map created with the effect of newly added indicators are given in Figs. 10 and 11.

When this change is encountered with the $SQI_{original}$ values, it has been determined that the new three indicators differentiate the SQI values. However, a relationship was still determined between the $SQI_{original}$ values and the $SQI_{modified}$ ($R^2 = 0.45$) (Fig. 12). In addition, the quality and moisture of the soil are a crucial factor in the structure, function, and diversity of karst ecosystems (Wang et al. 2005).

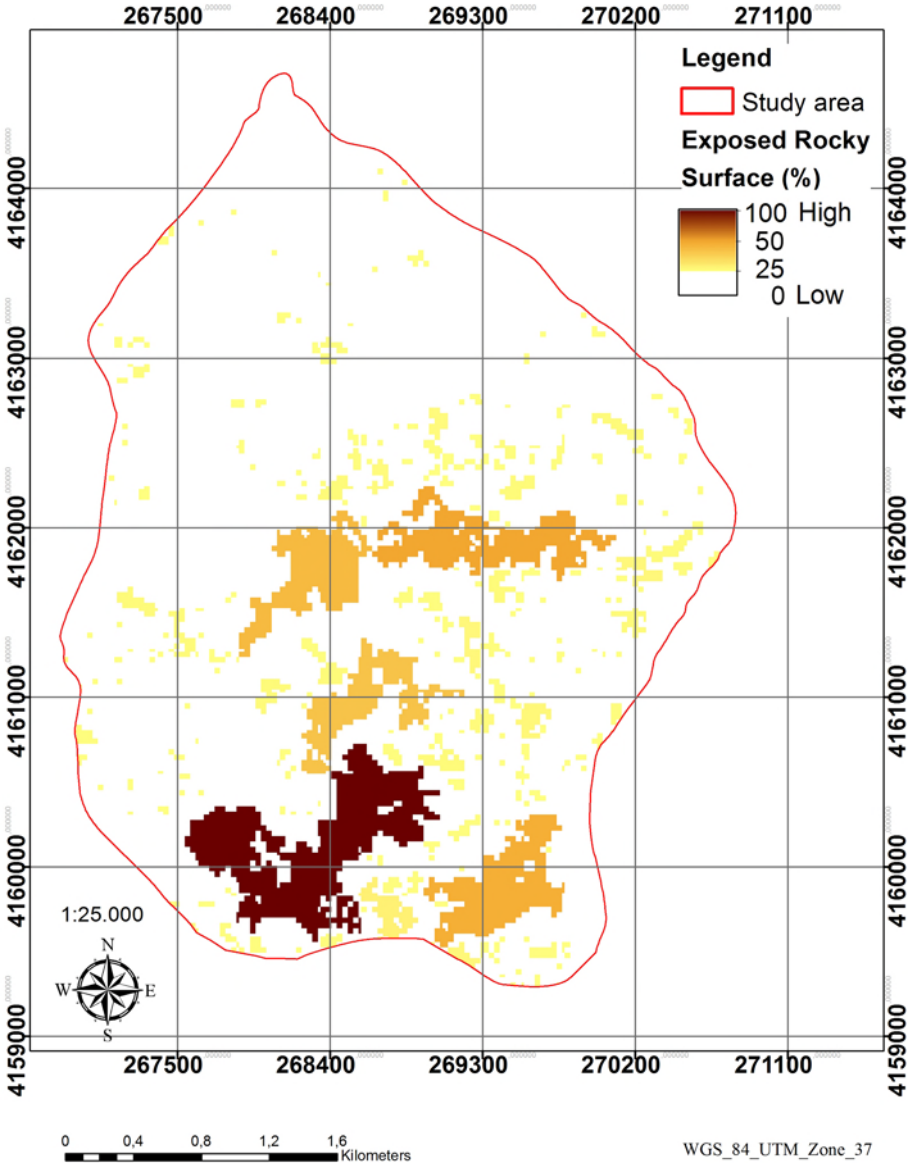

Fig. 6 Distribution map of exposed rocky surface

On the vegetation quality index map, the dominant effect of forest ecosystems located in the North-East aspect is observed (Fig. 13). On the management quality map, a change is observed depending on the land-use types (forest, agriculture, and rangeland (Fig. 14). The climate quality index does not change in the local area, thus climate parameters (rainfall and aridity) have a homogeneous effect in the study area (CQI = 1.41).

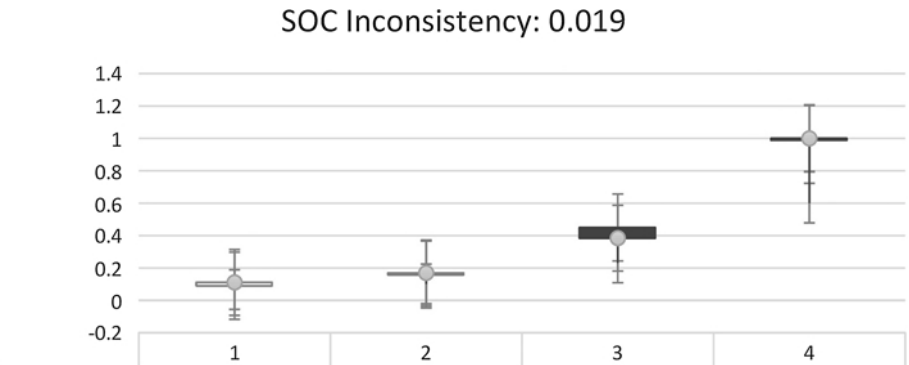

	1	2	3	4
Value	0.09	0.16	0.45	1
Normalized	0.066483478	0.101611339	0.230886864	0.601018318
Idealized	0.110618057	0.169065295	0.384159445	1

Fig. 7 Subcriterion SOC

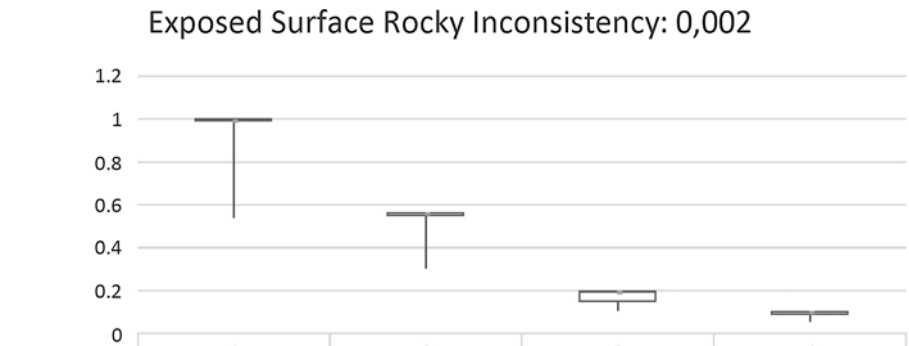

	1	2	3	4
Value	1	0.55	0.15	0.09
Normalized	0.538113898	0.302454156	0.105293435	0.054138512
Idealized	1	0.562063454	0.195671279	0.100607904

Fig. 8 Subcriterion exposed surface rocky

3.3 Environmentally sensitive area index for desertification in the karst ecosystem

In this study, $SQI_{modified}$ values specific to Karstic ecosystems produced by the AHP method were included in the ESAI calculation. Depending on the change in the SQI distribution in the area, there have been variations in the distribution in the ESAi map. When the $ESAi_{original}$ and $ESAi_{modified}$ maps are compared, it can be seen visually that the modified ESAi map is more detailed (Figs. 15 and 16).

Subtype **P** (potential areas) with an area of 51.15 ha (3.58%) has fine-textured, stony, deep, and well-drained soils, generally located in the north aspect. Karst area is characterized by low fire risk because of rocky surfaces. In a study conducted by Boudjemline and Semar, (2018) using MEDALUS method in Algeria, the ESAi map

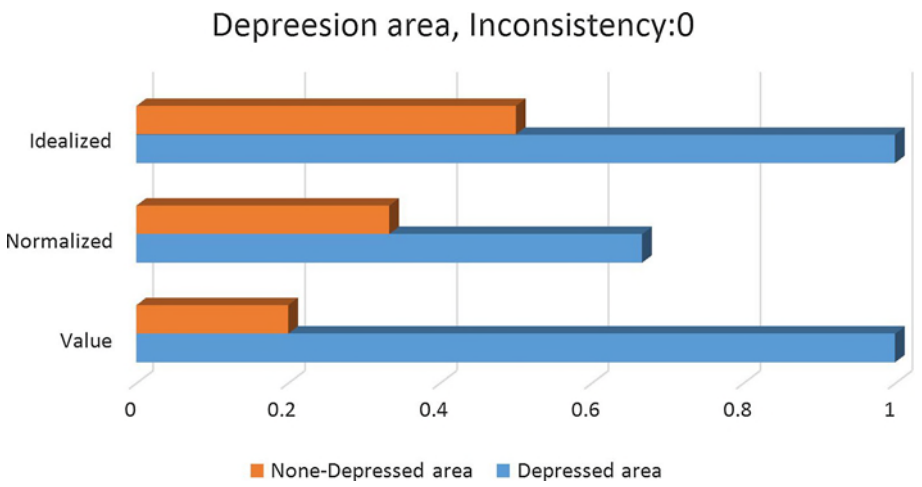

Fig. 9 Subcriterion depression area

Table 7 Exposed rocky surface index

Exposed rocky surface		
SQI Class	Cover rate	Index
Very high	0–25 (%)	0.20
High	25–50 (%)	0.36
Medium	50–75 (%)	1.03
Low	75–100 (%)	2.00

Table 8 Soil organic carbon content index

Soil Organic Carbon Content		
SQI Class	Rate (%)	Index
Very high	> 5	0.23
High	3–5	0.61
Medium	1–3	1.40
Low	0–1	2

Table 9 Depression area index

Depression areas		
SQI Class		Index
High	Depression area	0.99
Low	None Depression area	2.00

Table 10 Models and model parameters for the geo-statistical analyses

Parameters	Model	Regression function	Nugget, Co	Range, A	Sill, Co + C	ME	RMSSE	SDP
SQI	Circular	0.39172* x + 0.79	0.007	1827	0.02	0.02	0.93	Good
VQI	Exponential	0.42094* x + 0.88	0.007	2874	0.03	0.0005	1.01	Powerful
MQI	Spherical	0.46701* x + 0.66	0.07	3072	0.46	0.01	0.94	Powerful

ME Mean standard error, *RMSSE* Estimated standardized mean of error of mean square root, *SDP* Spatial dependence power

was created and it was determined that more than half of the Hodna basin soils were classified as "potential" less sensitive.

Subtype **F1** (fragile areas) have 184.97 ha (12.93%) with a moderate-textured, stony, moderate to deep, imperfectly drained soil. The climate is characterized mainly as sub-humid > 700 mm and a very dry bio-climatic index (BAI > 150). Subtype fragile (F1) areas are generally located in the east and west aspects. Subtype **F2** (fragile areas) have 269.4 ha (18.83%) areas with moderately textured, stony, moderate to deep, imperfectly drained soil. Fragile (F1) subtype areas generally located in the east and west aspects. Subtype **F3** (fragile areas) has 288.64 ha (20.18%) in the area with moderately textured, stony, moderate to deep, imperfectly drained soils. Subtype fragile (F1) areas are generally located in the east and south aspects.

Subtype **C1** (critical) have 235.41 ha (16.45%), and Subtype **C2** (critical) 344.77 ha (24.10%). Subtype **C3** (critical) have 56.3 ha (3.94%) and are areas with very poorly textured, very stony, very shallow, poorly drained soils. Subtype fragile (C1, C2, and C3) areas are generally located in the south aspect. The climate of the study area is characterized mainly as sub-humid > 700 mm and a very dry bio-climatic index (BAI > 150). Generally, these areas are due to wrong land use and the lowest enforced environmental protection policy owing to their lack of productivity (Fig. 16 and Table 11).

Karst areas on the limestone bedrock, because of the creation of shallow soils and poor water holding capacity, affect the soil quality negatively. These areas can cause excessively Fragile and Critical subtype fields to occur (Kosmas et al., 1993). The aspect with physiographic characteristics affects the fragile and critical sensitive areas greatly. The quality of the vegetation in the north aspect is higher than on the other side (Poesen et al., 1998). The sustainability of soil quality in karstic areas and its spread of soil fertility to the general area is very important for combat desertification. There are drought, flood, soil erosion, and soil nutrient problems in many karstic regions (Zhang et al., 2006). During the rocky desertification processes in the karstic areas, the loss of soil moisture causes a decrease in soil functions by reducing the soil quality and fertility (Chen & Wang, 2008).

When this change is encountered with the $ESA_{original}$ values, it has been determined that the new three indicators differentiate the ESAi values. However, a powerful relationship was still determined between the $ESA_{original}$ values and the $ESA_{modified}$ ($R^2 = 0.89$) (Fig. 17).

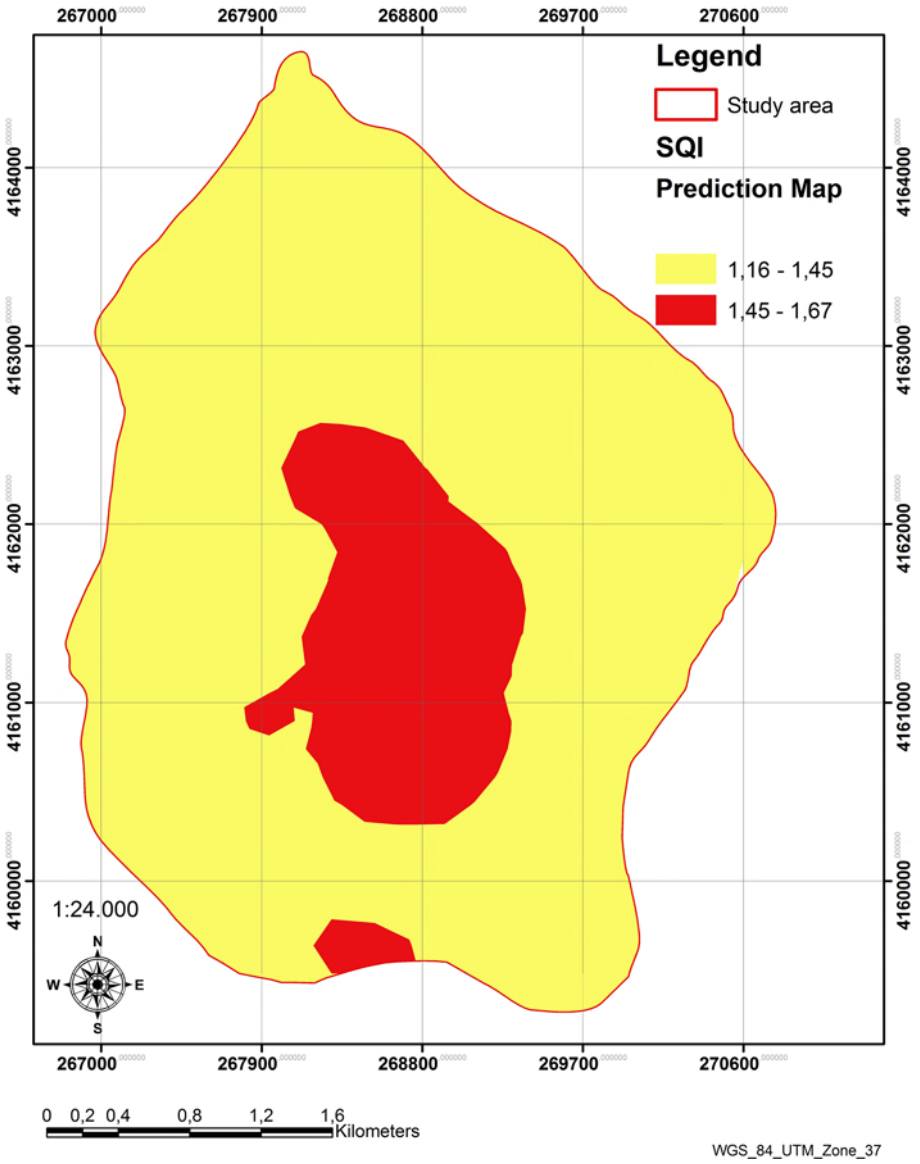

Fig. 10 Soil quality index map (Original)

3.4 $ESAi_{modified}$ and land use

An evaluation of the $ESAi_{modified}$ in view of land use type, ecological sensitivity was the lowest for all of the forest-covered areas (Tables 12 and 13). The regression equation defined for Potential (P) $ESAi_{modified}$ and the forest class type is $Y = -9.4361x + 52.963$ and $R^2 = 0.61$. Fragile ecological sensitivity area (F1) covers 39.75%, Fragile (F2) area covers 60.25% and the identified forest cover class is 10–40% (Tables 11 and 12). The regression

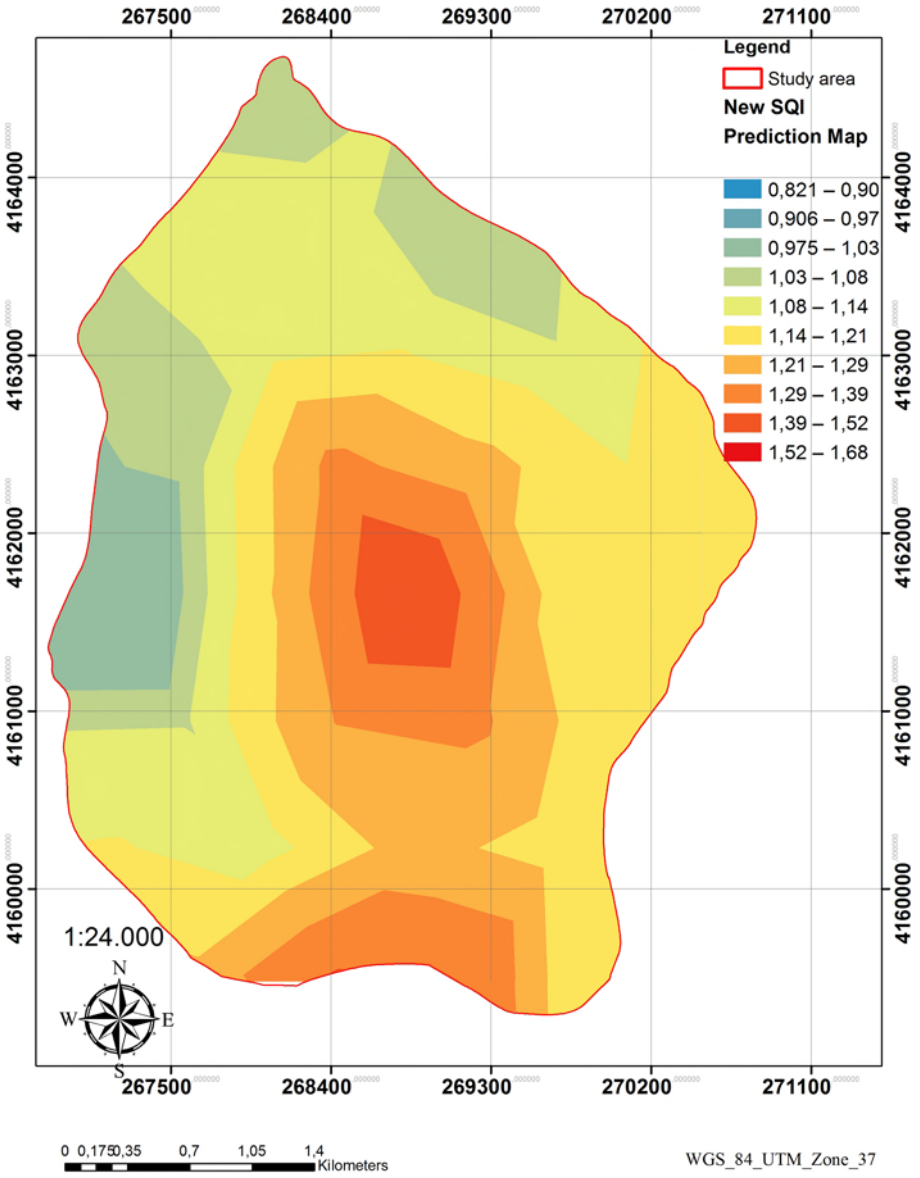

Fig. 11 Soil quality index map (Modified)

function between $ESAi_{modified}$ and the forest class type is $Y = -16.273x + 111.67$ and $R^2 = 0.18$. Fragile ecological sensitivity area (F2) covers 23.55%, Fragile (F3) area covers 76.45% and the identified forest cover class is 0–10% (Tables 11 and 12). The regression function between $ESAi_{modified}$ and the degraded forest class type is $Y = -2.25x + 47.214$ and $R^2 = 0.004$. Fragile ecological sensitivity area (F3) covers 28.46%, Critical (C1) area covers 30.56%, Critical (C2) area covers 29.55% and Critical (C3) area covers 11.43% of the agricultural area (Tables 12 and 13). The regression function between $ESAi_{modified}$ and

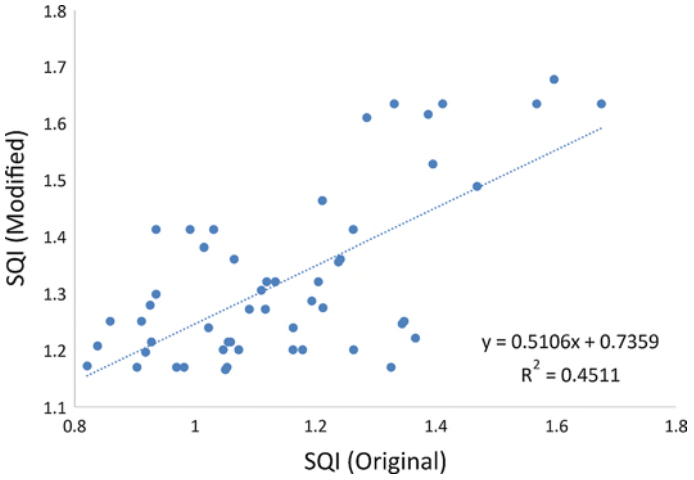

Fig. 12 Relationship between original SQI and modified SQI

the agricultural area is Y = 13.087x−10.113 and $R^2 = 0.41$. Roxo et al. (1999) found that the critical land with high ecological sensitivity is generally the agricultural fields near the settlement area. Images from settlement areas and degraded forest areas classified with fragile sensitivity (Fig. 18a, b).

Critical ecological sensitivity (C2) area covers 76.20% and Critical (C3) area covers 23.80% of the rangeland (Tables 12 and 13). The regression function between $ESAi_{modified}$ and the rangeland is $Y = 4.03x–8.9171$ and $R^2 = 0.36$. The rangeland has not enough water in the critical period, and fire and overgrazing have been much affected by drought (Clark, 1996). Intensive human activities affected desertification, especially in the Karst region (Zhang & Zhou, 2001; Mick, 2010; Jiang et al., 2014). Critical ecological sensitivity (C1) area covers 38.73%, Critical (C2) area covers 58.47% and Critical (C3) area covers 2.81% of the rocky land (Tables 12 and 13). The regression function between $ESAi_{modified}$ and the rocky land is $Y = 21.949x–34.289$ and $R^2 = 0.27$. All the settlement areas have been identified as having Fragile ecological sensitivity (F2) (Tables 10 and 11). The regression function between $ESAi_{modified}$ and the settlement area is $Y = -0.3554x + 2.8429$ and $R^2 = 0.04$). Complex karst topography has advantages and disadvantages. In karst ecosystems, sloping cropland is very small in size and highly variable among exposed rocks and water bodies. However, this complexity of karstic topography increases the diversity of microhabitats. The dynamic structure of the topography also influences the spatial distribution of $ESAi_{modified}$ variations (Descroix et al., 2001). Rehabilitation affecting conditions of land management and soil productivity (soil organic matter, texture, structure) can lead to an improvement in soil quality (Williams et al., 1983). The restoration process should be planned according to the ecology sensitivity areas such as "Potential" $ESAs_{(P)}$ "Fragile" $ESAs_{(F)}$ and "Critical" $ESAs_{(C)}$ classes in the Karst ecosystems. Except for the depression areas, shallow soil depth and high surface stoniness lead to negative site conditions for plant survival. If plant species selected according to ecological sensitivity, the restoration success rate will be increased (Dindaroglu, 2015). In the Mediterranean region, which is locally affected by desertification processes, the vulnerability of the land to degradation is affected by key environmental factors (climate, soil, vegetation, land use). Land

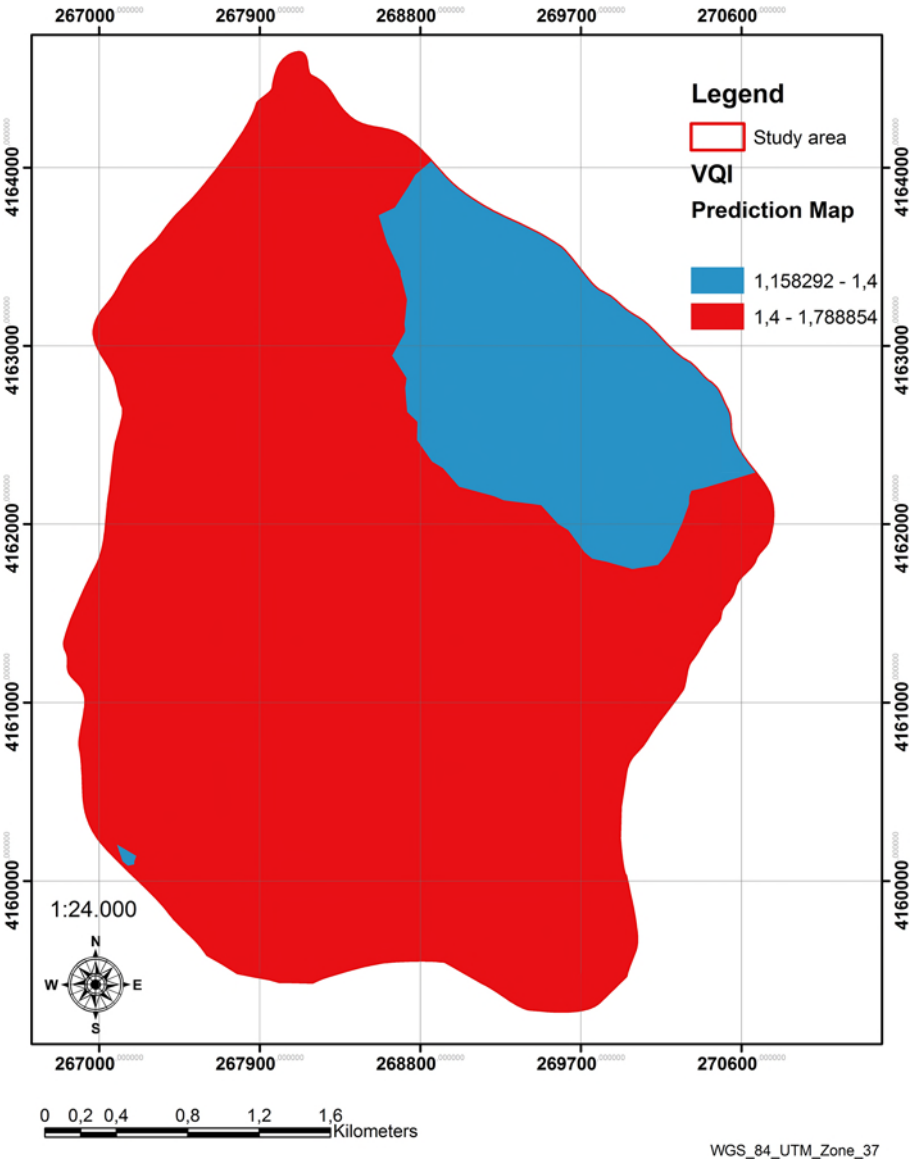

Fig. 13 Vegetation quality map

sensitivity classification has been identified as a possible target for mitigation strategies against desertification in land classified as highly fragile (Salvati, 2014). Models such as MEDALUS constitute the main basic issues to be taken into account in managing projects to be implemented rehabilitation measures and decontamination actions (Besser & Hamed, 2021).

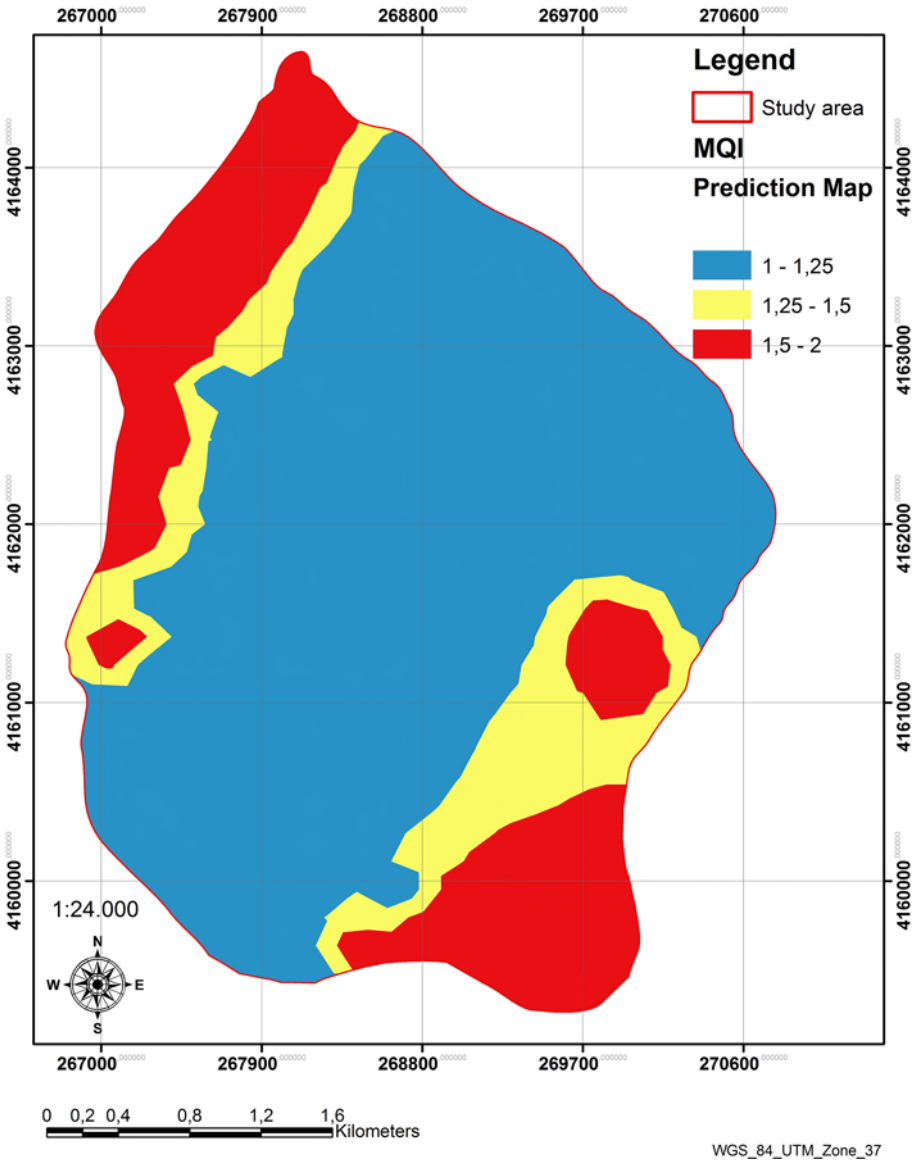

Fig. 14 Management quality map

3.5 Validation of $ESAi_{modified}$ in the karst ecosystem

Accuracy assessments of new indices of environmentally sensitive areas have been made using Field studies, satellite images (Googleearth), and Forest Management Plans (1/25,000). A total of 270 control points were determined using the randomized sampling method. Checkpoints have been imported into Google Earth using the KML format

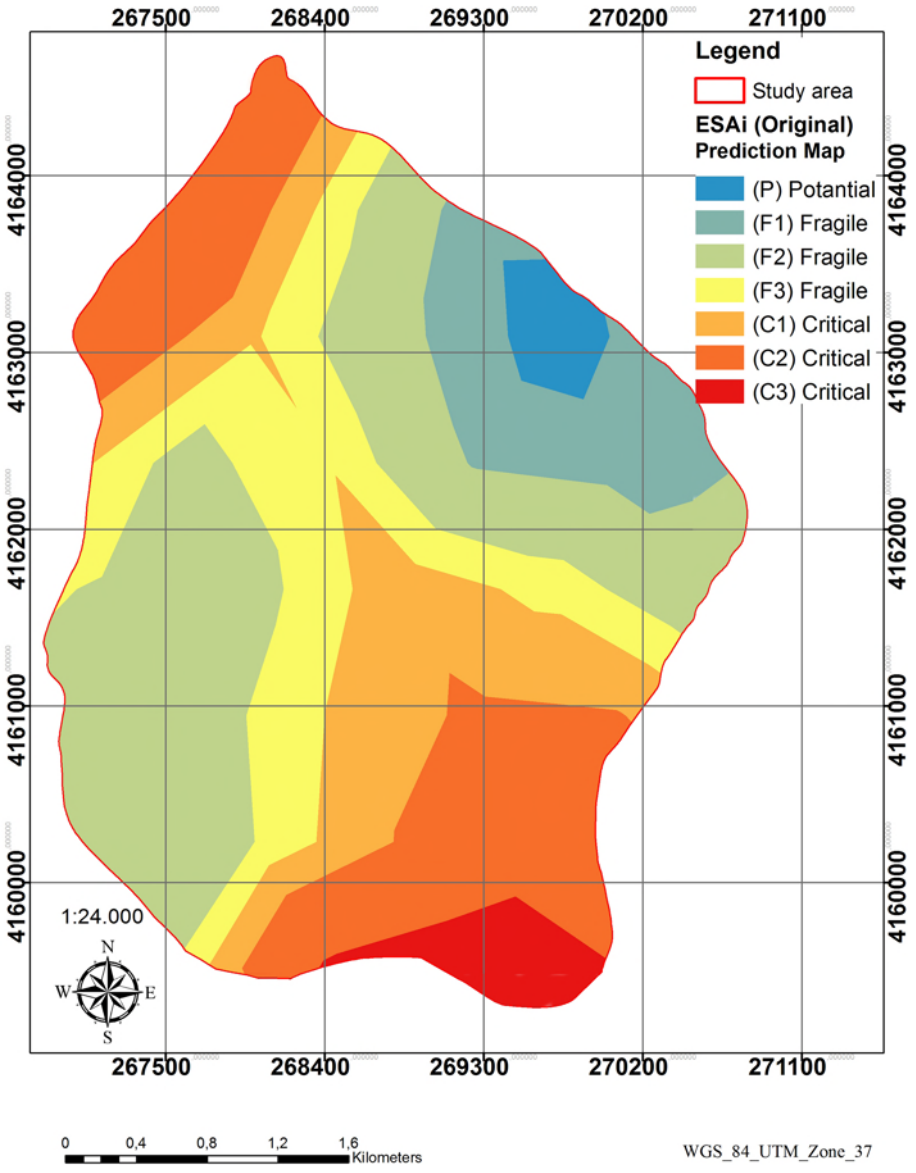

Fig. 15 ESAi (Original)

(Fig. 19). A total of 219 control points were confirmed. In general, 81.11% of control points were evaluated as correct, while 18.89% were evaluated as wrong. Points considered incorrect are generally located in transition areas (ecotones).

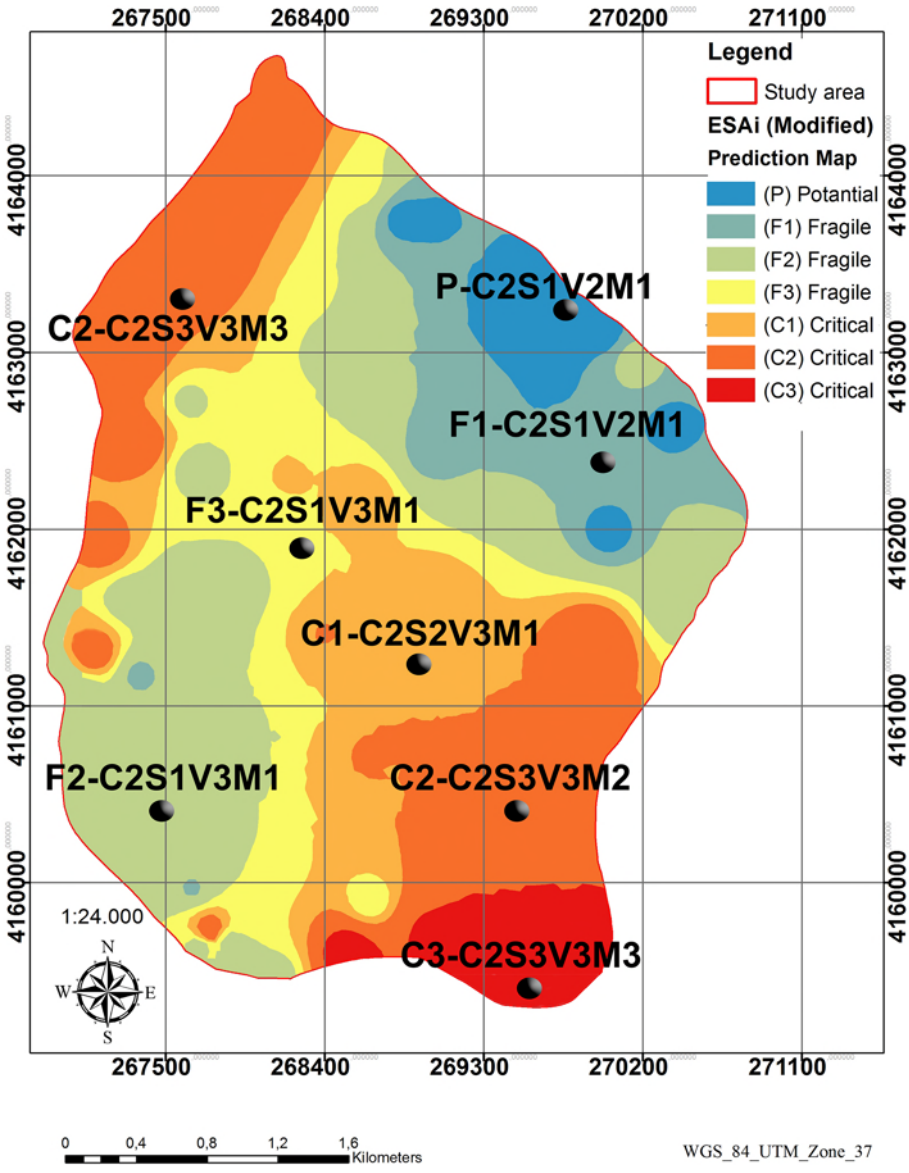

Fig.16 ESAi (Modified)

3.6 Limitations of the AHP process adopted for the karst ecosystem

The AHP Method has many advantages as well as disadvantages. According to Ramanathan (2001), when the AHP method is applied, the expression of subjective judgments with clear numbers may cause mistakes. In addition, too many comparing factors and binary matrices may cause errors during scoring. The ESAi map was produced by

Table 11 Spatial distribution of the $ESAi_{modified}$ type

ESAi Type	Subtype		
		Area (ha)	%
Potential	P	51.15	3.58
Fragile	F1	184.97	12.93
	F2	269.4	18.83
	F3	288.64	20.18
Critical	C1	235.41	16.45
	C2	344.77	24.10
	C3	56.3	3.94
Total		1430.64	100.00

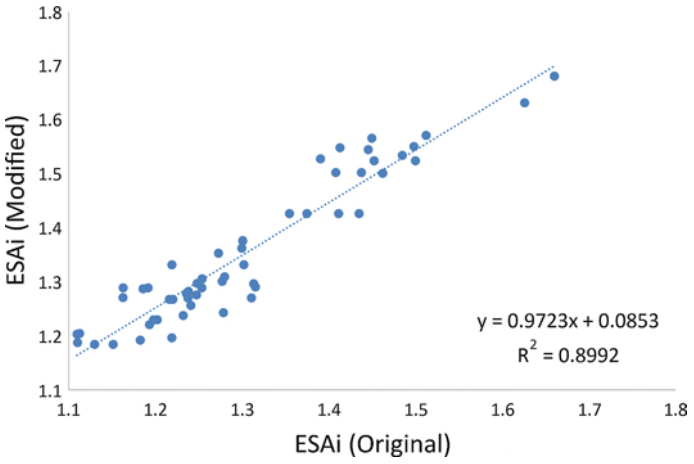

Fig. 17 Relationship between original SQI and modified SQI

Table 12 Land use type and $ESAi_{modified}$ type

$ESAi_{modified}$ Type	Subtype	Forest Cover Class %			Agriculture	Rangeland	Rocky	Settlement	Total
		40–100	10–40	0–10					
		Ha	Ha	Ha	Ha	Ha	Ha	Ha	Ha
Potential	P	51.15	0.00	0.00	0	0.00	0	0	51.15
Fragile	F1	55.38	129.59	0.00	0	0.00	0	0	184.97
	F2	0	196.45	63.00	0	0.00	0	9.95	269.4
	F3	0	0	204.5	84.14	0	0	0	288.64
Critical	C1	0	0	0	90.36	0	145.05	0	235.41
	C2	0	0	0	87.35	38.42	219	0	344.77
	C3	0	0	0	33.79	12	10.51	0	56.3
Total		106.53	326.04	267.5	295.64	50.42	374.56	9.95	1430.64

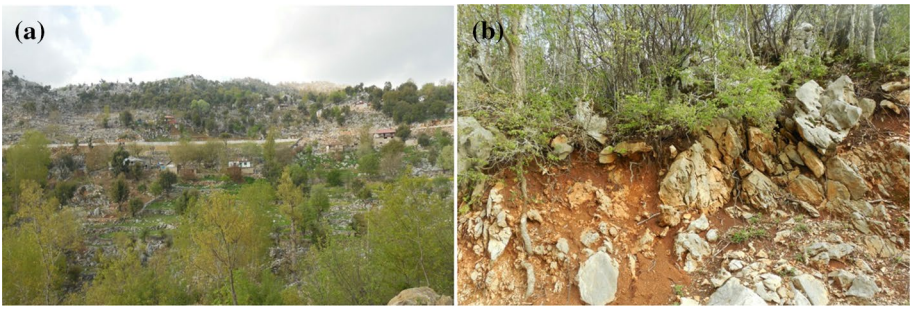

Fig. 18 Settlement area **a** and limestone formation **b** in the karstic ecosystem in the ESAi "Fragile Class"

Table 13 Land use type and $ESAi_{modified}$ type rates

$ESAi_{modified}$ Type	Subtype	Forest Cover Class %			Agriculture	Rangeland	Rocky	Settlement	Total
		40–100	10–40	0–10					
		%	%	%	%	%	%	%	%
Potential	P	48.01	0.00	0.00	0.00	0.00	0.00	0.00	3.58
Fragile	F1	51.99	39.75	0.00	0.00	0.00	0.00	0.00	12.93
	F2	0.00	60.25	23.55	0.00	0.00	0.00	100.00	18.83
	F3	0.00	0.00	76.45	28.46	0.00	0.00	0.00	20.18
Critical	C1	0.00	0.00	0.00	30.56	0.00	38.73	0.00	16.45
	C2	0.00	0.00	0.00	29.55	76.20	58.47	0.00	24.10
	C3	0.00	0.00	0.00	11.43	23.80	2.81	0.00	3.94
Total		100	100	100	100	100	100	100	100

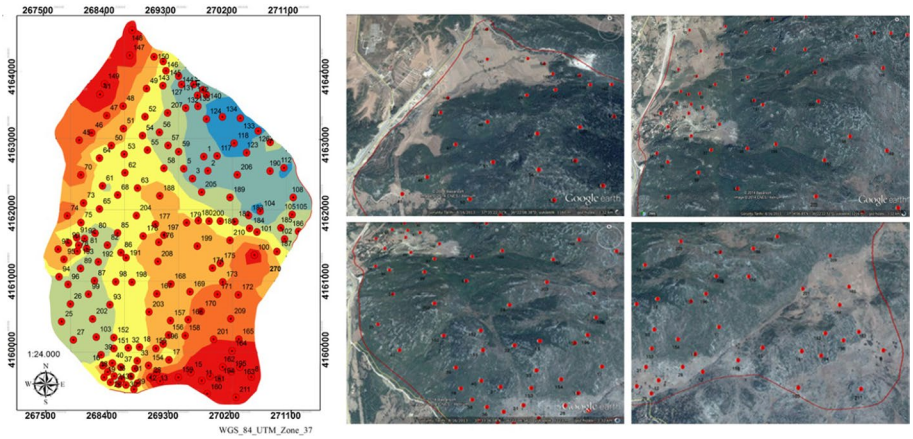

Fig. 19 Extracted control points from the $ESAi_{modified}$ map imported in Google Earth for visual validation

using the indicators obtained by various techniques together in this study. With the AHP technique, three new indices specific to karst ecosystems were added to the MEDALUS methodology using the results of field surveys and laboratory analyses. Finally, it was determined that the success rate in the accuracy tests of the produced ESAi distribution maps was 81.11%. However, it was not possible to evaluate the effects of the used new techniques on areas that were evaluated as wrong (18.89%) (Fig. 19).

4 Conclusions

Depending on the components of each ecosystem, the sensitivity factors are different. Therefore, determining the relationship between the factors with easy, cheap, and reliable methods will provide significant advantages in terms of planning and implementation. In this study, weights of important factors to Karst ecosystems such as soil organic carbon, depression area, exposed surface rocky have been investigated by the AHP method and, then ESAi distribution has been successfully mapped. A high correlation was found between $ESAi_{orginal}$ and $ESAi_{modified}$, as well as an ESAi distribution map specific to karstic ecosystems was produced. The index parameters added in this study are only related to SQI. However, in the end, $SQI_{modified}$ affected the ESAi distribution. The new SQI map produced with new indices specific t karstic ecosystems using AHP has revealed a more detailed spatial distribution. In addition, AHP, which includes new indices for different ecosystems, can be created and evaluated with many parameters. With this approach, more successful results can be obtained in the planning, management, and implementation activities in karstic natural ecosystem.

Forest areas and stand closures have significantly affected ecological sensitivity. Rangelands were vulnerable at the most critical level in the study area. The reason is related to the lack of enough productive rangeland in Karst areas and the overgrazing problem. Cropland has been found to be more sensitive (C3 critical level) than the rocky surface. Croplands show how human intervention can negatively affect ecological sensitivity in the karstic area. In the management of karst ecosystems in combating desertification, underground formations, groundwater systems, geomorphological, ecological, and hydrological relationships should be taken into account.

Acknowledgement The authors thank to Kahramanmaras Sutcu Imam University, Faculty of Forestry, Soil Science & Ecology laboratory.

References

Agnihotri, D., Kumar, T., & Jhariya, D. (2021). Intelligent vulnerability prediction of soil erosion hazard in semi-arid and humid region. *Environment, Development and Sustainability, 23*, 2524–2551.

Akbari, M., Memarian, H., Neamatollahi, E., Shalamzari, M. J., Noughani, M. A., & Zakeri, D. (2020). Prioritizing policies and strategies for desertification risk management using MCDM–DPSIR approach in northeastern Iran. *Environment, Development and Sustainability, 23*, 2503–25231.

Aksu, G. A., & Küçük, N. (2020). Evaluation of urban topography–biotope–population density relations for Istanbul-Beşiktaş urban landscape using AHP. *Environment, Development and Sustainability, 22*(2), 733–758.

Bai, X. Y., Wang, S. J., & Xiong, K. N. (2013). Assessing spatial temporal evolution processes of karst rocky desertification land: indications for restoration strategies. *Land Degradation & Development, 24*, 47–56.

Basu, T., & Pal, S. (2020). A GIS-based factor clustering and landslide susceptibility analysis using AHP for Gish River Basin, India. *Environment, Development and Sustainability, 22*, 4787–4819.

Besser, H., & Hamed, Y. (2021). Environmental impacts of land management on the sustainability of natural resources in Oriental Erg Tunisia, North Africa. *Environment, Development and Sustainability*. https://doi.org/10.1007/s10668-020-01135-9.

Blumenthal, M. (1947). Geology of Taurus Mountains at the hinterland of Seydişehir-Beyşehir: MTA Publ., ser. D, 2, Ankara.

Botoni, E., Larwanou, M., & Reij, C. (2010). La régénération naturelle assistée (RNA): une opportunité pour reverdir. *de la Grande Muraille Verte*, IRD Editions, pp. 151-162

Boudjemline, F., & Semar, A. (2018). Assessment and mapping of desertification sensitivity with MEDALUS model and GIS – Case study: basin of Hodna, Algeria. *Journal of Water and Land Development, 36*, 17–26.

Bouyoucos, G. J. (1962). Hydrometer method improved for making particle size analyses of soils. *Agronomy Journal, 54*, 464–465.

Budak, M., Günal, H., Çelik, İ, Yıldız, H., Acir, N., & Acar, M. (2018). Environmental sensitivity to desertification in northern Mesopotamia; application of modified MEDALUS by using analytical hierarchy process. *Arabian Journal of Geosciences, 11*(17), 481.

Cabral, A. C., De Miguel, J. M., & Rescia, A. J. (2003). Shrub encroachment in Argentinean savannas. *Journal of Vegetation Science, 14*(2), 145–152. https://doi.org/10.1658/1100-9233(2003)014[0145:SEIAS]2.0.CO;2.

Chen, H. S., & Wang, K. L. (2008). Soil water research in karst mountain areas of southwest China. *Research of Agricultural Modernization, 29*(6), 734–738.

Clark, S. C. (1996). Mediterranean ecology and an ecological synthesis of the field sites. In J. Brandt & J. Thornes (Eds.), *Mediterranean desertification and land use.* (pp. 271–299). New York: John Willey & Sons.

D'Antonio, C. M., & Vitousek, P. M. (1992). Biological invasions by exotic grasses, the grass/fire cycle, and global change. *Annual Review of Ecology and Systematics, 23*, 63–87.

Descroix, L., Viramontes, D., Vauclin, M., Barrios, J. L. G., & Esteves, M. (2001). Influence of soil surface features and vegetation on runoff anderosion in the Western Sierra Madre (Durango, Northwest Mexico). *CATENA, 43*, 115–135.

Dindaroglu, T. (2015). Resistance to the reclamation of environmentally sensitive areas through the establishment of a new forest ecosystem. *Fresenius Environmental Bulletin, 24*(4), 1195–1203.

Dindaroglu, T. (2020). Determination of ecological networks for vegetation connectivity using GIS & AHP technique in the Mediterranean degraded karst ecosystems. *Journal of Arid Environments*. https://doi.org/10.1016/j.jaridenv.2020.104385.

Dindaroglu, T., Gundogan, R., & Karaoz, M. O. (2019). Determination of spatial distribution of topsoil organic carbon stock using geostatistical technique in a karst ecosystem. *International Journal of Global Warming, 19*(3), 251–266.

Dindaroğlu, T., & Vermez, Y. (2019). Classification and mapping of some site features of karst ecosystems (Sarımsak Mountain Andırın-Kahramanmaraş). *Turkish Journal of Forest Science, 3*(1), 60–83.

DISMED (2005). http://dismed.eionet.eu.int/ Desertification information system for the Mediterranean

Dregne H.E, Chou N.T. (1992) Global desertification dimensions and costs. In: Dregne, H.E. (Ed.). *Degradation and restoration of arid lands*, Texas, Tech. University, Lubbock. pp. 249–282

ESRI. (2011). *Arcgis desktop: release 10.* . Environmental Systems Research Institute.

Febles, G. J., Vega, C. M., Tolón, B. A., & Lastra, B. X. (2012). Assessment of soil erosion in karst regions of Havana, Cuba. *Land Degradation and Development, 23*, 465–474.

Feoli, E., Giacomich, P., Mignozzi, K., Ozturk, M., & Scimone, M. (2003). Monitoring desertification risk with an index integrating climatic and remotely-sensed data: An example from the coastal area of Turkey. *Management of the Environmental Quality, 14*, 10–21.

Ferrara, A., Salvati, L., Sateriano, A., & Nole, A. (2012). Performance evaluation and costs assessment of a key indicator system to monitor desertification vulnerability. *Ecological Indicators, 23*, 123–129.

Gonzalez, P. (2001). Desertification and a shift of forest species in the West African Sahel. *Climate Research, 17*, 217–228.

Griffiths, J. C., & Dushenko, W. T. (2011). Effectiveness of GIS suitability mapping in predicting ecological impacts of proposed wind farm development on Aristazabal Island, BC. *Environment, Development and Sustainability, 13*(6), 957–991.

Gulcur, F., (1974). The Book of Physical and Chemical Analysis Methods of Soil. Kutulmus Printing House, IU Publication No. 1970, Faculty of Forestry Publication No. 201, Istanbul, 225 p.

Guo, F., Jiang, G., Yuan, D., & Polk, J. (2013). Evolution of major environmental geological problems in karst areas of southwestern china. *Environmental Earth Sciences, 69*(7), 2427–2435.

Haktanır, K., Karaca, A., & Omar, S. M. (2004). The prospects of the impact of desertification on Turkey, Lebanon, Syria and Iraq. In A. Marquina (Ed.), *Environmental Challenges in the Mediterranean 2000–2050, Chapter 9.* (pp. 139–154). Kluwer Academic Publishers.

Hamdouch, A., & Zuindeau, B. (2010). Sustainable development, 20 years on: methodological innovations, practices and open issues. *Journal of Environmental Planning and Management, 53*(4), 427–438.

Hornero, J., Manzano, M., Ortega, L., & Custodio, E. (2016). Integrating soil water and tracer balances, numerical modelling and GIS tools to estimate regional groundwater recharge: application to the Alcadozo Aquifer System (SE Spain). *Science of the Total Environment, 568*, 415–432.

Huang, Q. H., & Cai, Y. L. (2007). Spatial pattern of karst rock desertifi- cation in the middle of Guizhou Province, Southwestern China. *Environmental Geology, 52*, 1325–1330.

Irmak, A. (1954). *Research methods of soil in the field and in the laboratory*. Istanbul Univ. Publications 599/27.

Jensen, S. K., & Domingue, J. O. (1988). Extracting topographic structure from digital elevation data for geographic information system analysis. *Photogrammetric Engineering and Remote Sensing, 54*, 1593–1600.

Jhariya, D. C., Kumar, T., Dewangan, R., Pal, D., & Dewangan, P. K. (2017). Assessment of groundwater quality index for drinking purpose in the Durg district, Chhattisgarh using Geographical Information System (GIS) and Multi-Criteria Decision Analysis (MCDA) techniques. *Journal of the Geological Society of India, 89*(4), 453–459.

Jiang, Z. C., Lian, Y. Q., & Qin, X. Q. (2014). Rocky desertification in Southwest China: impacts, causes, and restoration. *Earth Science Reviews, 132*, 1–12.

Johnston, K., Hoef, M., Krivoruchko, K., & Lucas, N. (2001). *Using ArcGIS geostatistical Analyst*. . ESRI.

Kosmas, C., Danalatos, N., Moustakas, N., Tsatiris, B., Kallianou, C. H., & Yassoglou, N. (1993). The impacts of parent material and landscape position on drought and biomass production of wheat under semi-arid conditions. *Soil Technology, 6*, 337–349.

Kosmas, C., Danalatos, N. G., & Gerontidis, S. (2000). The effect of land parameters on vegetation performance and degree of erosion under Mediterranean conditions. *CATENA, 40*, 3–17.

Kosmas, C., Kirkby, M. J., & Geeson, N. (Eds.). (1999). *The Medalus Project: Mediterranean desertification and land use: Manual on key indicators of desertification and mapping environmentally sensitive areas to desertification*. Directorate-General Science, Research and Development.

Kozlu, H. (1987). Misis-Andırın Dolaylarının Stratigrafisi ve Yapısal Evrimi. *Türkiye 7. Petrol Kong*., Ankara, pp. 104–116.

Langemeyer, J., Gómez-Baggethun, E., Haase, D., Scheuer, S., & Elmqvist, T. (2016). Environmental science & policy bridging the gap between ecosystem service assessments and land-use planning through multi-criteria decision analysis (MCDA). *Environmental Science & Policy., 62*, 45–56.

Liu, J., Gao, J., Ma, S., Wang, W., & Zou, C. (2015). Comprehensive evaluation of ecoenvironmental sensitivity in Inner Mongolia China. *China Environmental Science, 35*(2), 591–598.

Maidment, D. R. (2002). Arc Hydro, GIS for Water Resources. ESRI, Redlands, California, USA. Isbn: 1-58948034-1

Maidment, D. R., Djokic, D. (2000). Hydrologic and Hydraulic Modeling Support With Geographical Information Systems. Esri, Redlands, California, USA. Isbn: 927378100

MGM. (2017). General Directorate of State Meteorology Affairs, Kahramanmaraş Meteorology Provincial Directorate, Kahramanmaras - Andirin Meteorology Station Report Book, pp. 1975-2010

Mick, D. (2010). Human interaction with Caribbean karst landscapes: past, present and future. *Acta Carsologica, 39*, 137–146.

Nelson, D.W., Sommers, L. E. (1996). Total Carbon, Organic Carbon, and Organic Matter, Methods of Soil Analysis, Part 3. Chemical Methods, Ed: Sparks, D.L., Page, A.L., Helmke, P.A., Loeppert, R.H., Soltanpour, P.N., Tabatabai, M.A., Johnston, C.T., Sumner, M.E., *Soil Science Society of America*, 5, 961-1010

Okin, G. S., Murray, B., & Schlesinger, W. H. (2001). Degradation of sandy arid shrubland environments: observations, process modeling, and management implications. *Journal of Arid Environments, 47*, 123–144.

Peng, J., Xu, Y. Q., Zhang, R., Xiong, K. N., & Lan, A. J. (2013). Soil erosion monitoring and its implication in a limestone land suffering from rocky desertification in the Huajiang Canyon, Guizhou, Southwest China. *Environment and Earth Science, 69*, 831–841.

Poesen, J., van Wesemael, B., Bunte, K., & Benet, A. (1998). Variation of rock fragment cover and size along semiarid hillslopes: a book of case study from southern Spain. *Geomorphology, 23*, 323–335.

Puigdefabregas, J. (1998). Ecological impacts of global change on drylands and their implications on desertification. *Land Degradation and Rehabilitation, 9*, 393.

Ramanathan, R. A. (2001). Note on the use of the analytic hierarchy process for environmental impact. *Journal of Environmental Management, 63*, 27–35.
Rossi, R. (2020). Desertification and agriculture. European Parliamentary Research Service PE 646.171 https://www.europarl.europa.eu/RegData/etudes/BRIE/2020/646171/EPRS_BRI(2020)646171_EN.pdf
Roxo, M. J., Mourao, J., Rodrigues, M. L., & Casimiro, P. C. (1999). *Applicatıon of the proposed methodology for defining ESAs of the Alentejo region Metrola municipality*. .
Saaty, R.W., Rokou, E., Adams, W. J. (2019). Super Decisions Software development is sponsored by the Creative Decisions Foundation. Accessed Date: 10.12.2019. https://www.superdecisions.com/about/index.php?section=devTeam
Saaty, T. L. (1980). *The analytic hierarchy process*. . McGraw-Hill.
Saaty, T. L. (1990). How to make a decision: The analytic hierarchy process. *European Journal of Operational Research*, *48*(1), 9–26.
Saaty, T. L. (1991). *Método de Análise Hierárquica*. . São Paulo.
Saaty, T. L., & Vargas, L. G. (1994). *Decision making in economic, political, social, and technological environments with the analytic hierarchy process*. . RWS Publications.
Salvati, L. (2014). Toward a 'Sustainable'land degradation? Vulnerability degree and component balance in a rapidly changing environment. *Environment, Development and Sustainability, 16*(1), 239–254.
Seager, R. (2007). Model projections of an imminent transition to a more arid climate in southwestern North America. *Science, 16*(5828), 1181–1184.
Sharma, K. D. (1998). The hydrological indicators of desertification. *Journal of Arid Environments, 39*(2), 121–132.
Smith, P., Calvin, K., Nkem, J., Campbell, D., Cherubini, F., Grassi, G., Korotkov, V., Hoang, A. L., Lwasa, S., McElwee, P., Nkonya, E., Saigusa, N., Soussana, J. F., Taboada, M. A., Manning, C., Nampanzira, D., Navarro, C. A., Vizzarri, M., House, J., … Rounsevell, M. (2019). Which practices co-deliver food security, climate change mitigation and adaptation, and combat land degradation and desertification? *Global Change Biology, 26*(3), 1532–1575.
Symeonakis, E., Karathanasi, N., Koukoulas, S., & Panagopoulos, G. (2014). Monitoring sensitivity to land degradation and desertification with the environmentally sensitive area index: the case of Lesvos Island. *Land Degradation and Development, 22*, 184–197.
UNCCD. (1994). *United Nations Convention to Combat Desertification in Those Countries Experiencing Serious Drought and/or Desertification Particularly in Africa: United Nations Convention to Combat Desertification Text with Annexes*. . UNEP.
UNEP (2007). Natural Disasters and Desertification. United Nations Environment Programme. Post-Conflict *Environmental Assessment*. ISBN: 978-92-807-2702-9, p: 69
USGS (1997). United States Geological Survey article "Desertification" <http://pubs.usgs.gov/gip/deserts/desertification/> Maintained by Publications Service Center Last modified 10/29
Veni, G., DuChene, H., Crawford, N.C., Groves, C.G., Huppert, G.N., Kastning, E.H., Olson, R., Wheeler, B.J. (2001). Living With Karst. American Geological Institute, ISBN 0–922152–58–6
Walkley, A., & Black, I. A. (1934). An examination of the Degtjareff method for determining soil organic matter, and a proposed modification of the chromic acid titration method. *Soil Science*, *37*(1), 29–38.
Wang, D. L., Zhu, S. Q., & Huang, B. L. (2005). Internal Factors Influencing Karst Rocky Desertification (in Chinese). *J. Zhej. For. Coll., 22*, 266–271.
Williams, J., Prebble, R. E., Williams, W. T., & Hignett, C. T. (1983). The influence of texture, structure and clay mineralogy on the soil moisture characteristic. *Australian Journal of Soil Research, 21*, 15–32.
Wu, X., Liu, H., Huang, X., & Zhou, T. (2011). Human driving forces: Analysisof rocky desertification in karst region in guanling county, guizhou province. *Chinese Geographical Ence, 21*(5), 92–100.
Xu, E. Q., & Zhang, H. Q. (2014). Characterization and interaction of driving factors in karst rocky desertification: a case study from Changshun China. *Solid Earth, 5*, 1329–1340. https://doi.org/10.5194/se-5-1329-2014.
Yılmaz, Y., & Gurer, Ö. F. (1996). Andırın Kahramanmaraş dolayında Misis Andırın kuşağının jeolojisi ve evrimi. *Turkish Journal Of Earth Sciences, 5*, 39–55.
Zhang, D. F., & Zhou, D. Q. (2001). Intrinsic driving mechanism of land rocky desertification in karst regions of Guizhou Province. *Bulletin of Soil and Water Conservation, 21*, 1–5.
Zhang, P., Li, L., Pan, G., & Ren, J. (2006). Soil quality changes in land degradation as indicated by soil chemical, biochemical and microbiological properties in a karst area of southwest Guizhou China. *Environmental Geology, 51*(4), 609–619.
Zou, H., & Ma, X. (2021). Identifying resource and environmental carrying capacity in the Yangtze River Economic Belt, China: The perspectives of spatial differences and sustainable development. *Environment, Development and Sustainability*. https://doi.org/10.1007/s10668-021-01271-w.

Zuindeau, B. (2007). Territorial equity and sustainable development. *Environmental Values, 16*(2), 253–268.